Hetero-trinuclear near-infrared (NIR) luminescent Zn_2Ln complexes from Salen-type Schiff-base ligands†

Weiyu Bi,[a] Tao Wei,[a] Xingqiang Lü,*[ab] Yani Hui,[a] Jirong Song,[a] Shunsheng Zhao,[b] Wai-Kwok Wong*[b] and Richard A. Jones[c]

Received (in Gainesville, FL, USA) 31st May 2009, Accepted 10th August 2009
First published as an Advance Article on the web 22nd September 2009
DOI: 10.1039/b9nj00228f

With the Zn–Schiff-base **[ZnL^1(Py)]** or **[ZnL^2(Py)]** from the simple Salen-type Schiff-base ligand **H$_2$L^1** or **H$_2$L^2** (**H$_2$L^1**: *N*,*N*′-bis(salicylidene)ethylene-1,2-diamine; **H$_2$L^2**: *N*,*N*′-bis(salicylidene)phenylene-1,2-diamine) without the outer O_2O_2 portion as the precursor, two series of eight trinuclear Zn_2Ln arrayed complexes (Ln = Nd (**1** or **5**), Yb (**2** or **6**), Er (**3** or **7**) or Gd (**4** or **8**)) have been obtained by the further reaction with $Ln(NO_3)_3{\cdot}6H_2O$, respectively. The results of photophysical studies show that the strong and characteristic NIR luminescence with emissive lifetimes in microsecond ranges, has been sensitized from the excited state (^{1}LC and ^{3}LC or only ^{1}LC) of the ligand, whereas the Zn(II)-based visible luminescence is mostly quenched because of quite effective intramolecular energy transfer from the ligand-centered excited state of the Zn(II)–Schiff base complex to Ln(III) ions.

Introduction

Much recent effort has been devoted to near infrared (NIR) luminescent Ln^{3+} (Nd^{3+}, Yb^{3+} or Er^{3+}) complexes with long-lived and characteristic line like emission bands, because of their potential applications in fluoro-immunoassays,[1] organic light-emitting diodes (OLED)[2] and optical telecommunication.[3] However, due to forbidden parity from the f–f transitions,[4] the absorption coefficients of these lanthanide ions are normally very low ($\varepsilon \approx 1$–$10\ M^{-1}\ cm^{-1}$). Though many cyclic[5] or acyclic[6] aromatic ligands with fully allowed π–π* transitions in the UV region have been designed for overcoming the low light absorbance of Ln^{3+} ions, and it is becoming more difficult to find ligand-centered chromophores at wavelengths longer than the UV.[7] The best source of strongly absorbing chromophores spanning the visible region is the d-block metal complexes[8] (*i.e.* Cr(III),[9] Co(III),[10] Zn(II),[11] Ru(II),[12] Pd(II),[13] Pt(II),[14] Ir(III),[15] Au(I),[16] Ag(I),[17] Cd(II),[18] Re(I) or Os(II)[19]), which display absorption bands at almost any desired wavelength and the desired excited states (^{1}LC, ^{3}LC, ^{3}MLCT or ^{3}LMCT), and have been demonstrated to effectively transfer energy to Ln^{3+} ions indirectly.

There is currently growing interest in the synthesis and magnetic behavior[20] of d–f heteronuclear complexes from compartmental Salen-type Schiff-base ligands, while there are relatively few studies on the photophysical properties of these compounds. Focusing on the choice of Zn–Schiff-base complexes with intense and tunable absorption maxima in the visible region,[21] our past studies tried to use them as antennae or sensitizers (donors) for NIR luminescence of Ln^{3+} ions complexes (acceptors),[22] which show that the Salen-type Schiff-base ligands with outer O_2O_2 moieties from MeO groups are apt to bind both 3d Zn^{2+} and 4f Ln^{3+} ions, effectively preventing luminescent quenching arising from OH-, CH- or NH-oscillators of the solvates around the 4f ions.[23] To examine NIR luminescent properties, in addition to the changing of spacers or electronic properties of the substituents (large π-conjugated aromatic rings or heavy atom Br) on the flanking phenyl rings of Schiff-base ligands,[22] multinuclear heterometallic complexes have been constructed from functional bridges with OH[24] or anionic groups[25] and multidentate spacers with bipyridyl[26] or bicarboxylate ligands,[27] endowing enhanced NIR luminescent properties. While for the simple Salen-type Schiff-base ligands without the outer O_2O_2 portion, to the best of our knowledge, there has been no report on the d–f heterometallic complexes, despite much research on d-block complexes[28] or recent 4f ion complexes.[29] As a matter of fact, the input of MeO groups on the Salen-type Schiff-base ligands is not necessary to bind both 3d and 4f ions, because two or more Zn–Schiff-base complexes can further coordinate the same 4f ion from their phenolic O atoms, giving a feasible route to the construction of $(Zn)_n$-4f ($n \geq 2$) heterometallic complexes. On the other hand, from the viewpoint of improving NIR luminescence, having two or more energy donors may strengthen the sensitization process. Herein, with Zn–Schiff-bases **[ZnL^1(Py)]** or **[ZnL^2(Py)]** from the simple Salen-type Schiff-base ligands **H$_2$L^1** or **H$_2$L^2** as the precursor, two series of eight hetero-trinuclear Zn_2Ln arrayed complexes (Ln = Nd (**1** or **5**),

[a] *Shaanxi Key Laboratory of Degradable Medical Material, Shaanxi Key Laboratory of Physico-inorganic Chemistry, Northwest University, Xi'an 710069, Shaanxi, China. E-mail: lvxq@nwu.edu.cn*
[b] *Department of Chemistry, Hong Kong Baptist University, Waterloo Road, Kowloon Tong, Hong Kong, China. E-mail: wkwong@hkbu.edu.hk*
[c] *Department of Chemistry and Biochemistry, The University of Texas at Austin, 1 University Station A5300, Austin, TX 78712-0165, USA*
† Electronic supplementary information (ESI) available: Supplementary figures; spectra. CCDC reference numbers 725680 and 725681. For ESI and crystallographic data in CIF or other electronic format see DOI: 10.1039/b9nj00228f

Yb (**2** or **6**), Er (**3** or **7**) or Gd (**4** or **8**)) have been obtained by reacting the Zn–Schiff-base with $Ln(NO_3)_3{\cdot}6H_2O$. The syntheses, structures and photophysical properties of these heterometallic complexes are reported, and the sensitization and the energy transfer of the Zn(II)–Schiff-base complexes for the NIR luminescence of the 4f ions are also discussed.

Results and discussion

As shown in Scheme 1, the reaction of equimolar amounts of $\mathbf{H_2L^1}$ or $\mathbf{H_2L^2}$, $Zn(OAc)_2{\cdot}2H_2O$ and absolute pyridine (**Py**) in absolute MeOH or EtOH, afforded the respective precursor **[ZnL^1(Py)]** or **[ZnL^2(Py)]** in good yields of *ca.* 80%. Further reaction of the respective precursor **[ZnL^1(Py)]** or **[ZnL^2(Py)]** with $Ln(NO_3)_3{\cdot}6H_2O$ (**Ln** = **Nd**, **Yb**, **Er** or **Gd**) in 2 : 1 molar ratio resulted in the formation of hetero-trinuclear Zn_2Ln complexes **1–4** or **5–8**, respectively.

The eight complexes **1–8** are insoluble in water while more soluble in common organic solvents. These complexes were characterized by EA and FT-IR, and X-ray quality crystals were obtained for **1** and **5**. Selected crystal properties of complexes **1** and **5** are given in Tables 1–2. For complex **1**, as shown in Fig. 1, the four phenoxo oxygen atoms of the two **[ZnL^1(Py)]** components coordinate to one Nd(III) ion resulting in the formation of a trinuclear Zn_2Nd complex. Each Zn^{2+} (Zn1 or Zn2) ion has a five-coordinate environment and adopts a distorted square pyramidal geometry, as shown by the respective τ value[30] of 0.287 for Zn1 or 0.357 for Zn2 ion, composed of the inner N_2O_2 core from the Schiff-base $(\mathbf{L^1})^{2-}$ ligand as the base plane, and one N atom from the coordinated **Py** at the apical position, while the Nd^{3+} ion is in the outer sites, two doubly bridged Zn^{2+} ions by two phenoxo oxygen atoms of two Schiff-base $(\mathbf{L^1})^{2-}$ ligands with a Zn···Nd separation of 3.499(2) or 3.512(2) Å, respectively. The Nd^{3+} ion is nine coordinated. In addition to the four bridging phenoxo oxygen atoms, it completes its coordination environment with five oxygen atoms from two bidentate and one monodentate NO_3^- anions. The Nd–O bond lengths depend on the nature of the oxygen atoms: they vary from 2.422(9) to 2.625(11) Å, and the bond lengths from phenoxo

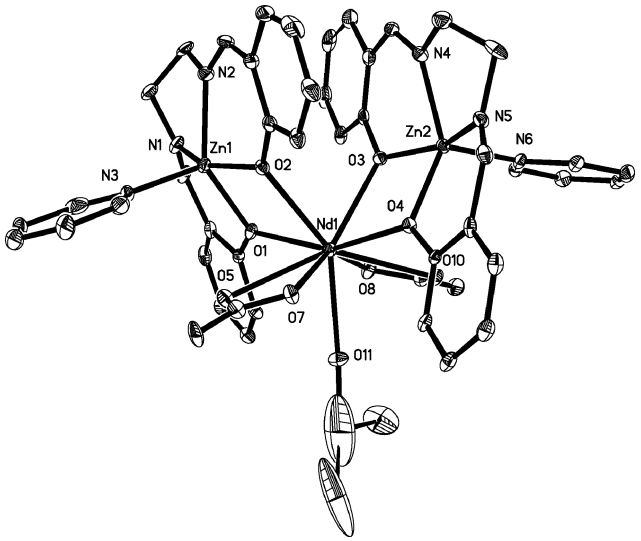

Fig. 1 Perspective drawing of compound **1**, H atoms and solvates are omitted for clarity.

oxygen atoms are shorter than those from oxygen atoms of NO_3^- anions. It should be noted that the formation of a trinuclear Zn_2Nd (**1**) array, is incomparable to that of binuclear ZnLn complexes[22] from the Salen-type Schiff-base ligands with the outer MeO sidearms. Furthermore, the occupation of **Py** at the axial position of 3d Zn^{2+} ions is considered to effectively avoid further coordination of solvents around the 4f ions.

The change of linker group from ethylene to phenylene ($\mathbf{H_2L^1}$ to $\mathbf{H_2L^2}$) did not lead to a significant change of the structure of the trinuclear complex **5**. As shown in Fig. 2, the respective Zn···Nd separation from two Zn^{2+} and Nd^{3+} ions bridged by four phenoxo oxygen atoms of two Schiff-base $(\mathbf{L^2})^{2-}$ ligands, is 3.504(1) or 3.521(1) Å. It is worth noting that both of the two five-coordinate Zn^{2+} ions in complex **5** have a slightly distorted square pyramidal geometry (as shown by the τ values of 0.03 for Zn1 or 0.047 for Zn2 ion), the Nd^{3+} ion in complex **5** is ten coordinated, composed of four phenoxo oxygen atoms from the two Schiff-base $(\mathbf{L^2})^{2-}$ ligands, and

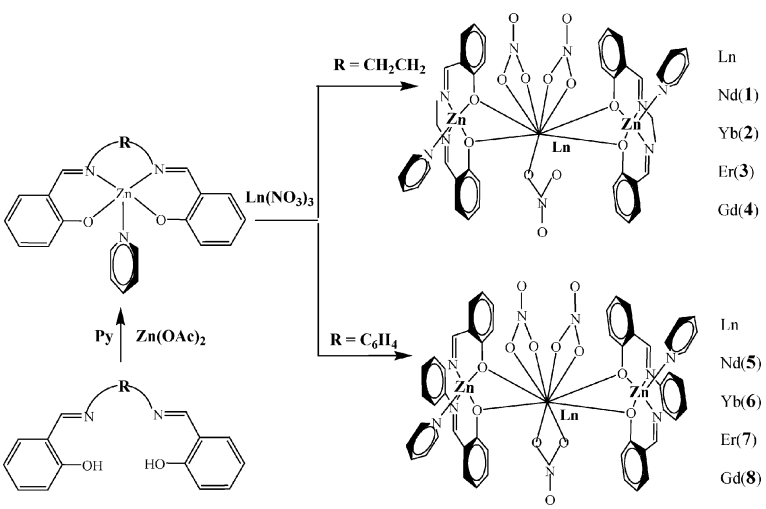

Scheme 1 Controlled design of trinuclear heterometallic 3d–4f complexes.

Table 1 Crystal data and refinement for complexes **1** and **5**

Compound	**1**	**5**
Empirical formula	$C_{42}H_{40}N_9O_{14}Zn_2Nd$	$C_{54}H_{48}N_9O_{14}Zn_2Nd$
Formula weight	1169.81	1321.99
Crystal system	Orthorhombic	Monoclinic
Space group	*Pna*2(1)	*Cc*
λ/Å	1.54184	0.71073
a/Å	21.4029(4)	14.654(4)
b/Å	11.2479(3)	19.038(5)
c/Å	18.8883(5)	19.859(7)
α/°	90	90
β/°	90	97.990(8)
γ/°	90	90
V/Å^3	4556.04(19)	5487(3)
Z	**4**	4
ρ/g cm^{-3}	1.702	1.600
Crystal size/mm	0.31 × 0.25 × 0.21	0.35 × 0.31 × 0.23
μ(Mo-Kα)/mm^{-1}	10.424	1.874
T/K	293(2)	273(2)
Data/restraints/parameters	4749/4/613	9512/2/721
Quality-of-fit indicator	1.056	0.874
Final R indices [$I > 2\sigma(I)$]	R_1 = 0.0439	R_1 = 0.0383
	wR_2 = 0.1258	wR_2 = 0.0807
R indices (all data)	R_1 = 0.0492	R_1 = 0.0620
	wR_2 = 0.1292	wR_2 = 0.0870

Table 2 Interatomic distances (Å) and bond angles (°) with esds for complexes **1** and **5**

1		**5**	
Zn(1)–N(1)	2.027(15)	Zn(1)–N(1)	2.074(5)
Zn(1)–N(2)	2.067(13)	Zn(1)–N(2)	2.042(5)
Zn(1)–N(3)	2.034(14)	Zn(1)–N(3)	2.092(6)
Zn(1)–O(1)	2.023(10)	Zn(1)–O(1)	2.017(4)
Zn(1)–O(2)	2.019(10)	Zn(1)–O(2)	1.999(5)
Zn(2)–N(4)	2.054(12)	Zn(2)–N(4)	2.060(6)
Zn(2)–N(5)	2.045(14)	Zn(2)–N(5)	2.058(6)
Zn(2)–N(6)	2.055(12)	Zn(2)–N(6)	2.047(6)
Zn(2)–O(3)	2.037(10)	Zn(2)–O(3)	2.008(5)
Zn(2)–O(4)	2.024(9)	Zn(2)–O(4)	2.020(4)
Nd(1)–O(1)	2.449(9)	Nd(1)–O(1)	2.439(4)
Nd(1)–O(2)	2.466(10)	Nd(1)–O(2)	2.538(4)
Nd(1)–O(3)	2.422(9)	Nd(1)–O(3)	2.567(5)
Nd(1)–O(4)	2.441(9)	Nd(1)–O(4)	2.409(4)
Nd(1)–O(5)	2.619(11)	Nd(1)–O(5)	2.564(5)
Nd(1)–O(7)	2.593(12)	Nd(1)–O(7)	2.631(5)
Nd(1)–O(8)	2.597(13)	Nd(1)–O(8)	2.625(5)
Nd(1)–O(10)	2.625(11)	Nd(1)–O(10)	2.640(5)
Nd(1)–O(11)	2.460(9)	Nd(1)–O(11)	2.528(5)
		Nd(1)–O(13)	2.697(6)
N(1)–Zn(1)–N(2)	79.4(7)	N(1)–Zn(1)–N(2)	79.9(2)
N(1)–Zn(1)–N(3)	103.0(6)	N(1)–Zn(1)–N(3)	100.0(2)
N(1)–Zn(1)–O(1)	90.2(5)	N(1)–Zn(1)–O(1)	89.56(19)
N(1)–Zn(1)–O(2)	156.9(5)	N(1)–Zn(1)–O(2)	150.4(2)
N(4)–Zn(2)–N(5)	80.5(6)	N(4)–Zn(2)–N(5)	79.6(2)
N(4)–Zn(2)–N(6)	111.7(6)	N(4)–Zn(2)–N(6)	104.7(2)
N(4)–Zn(2)–O(3)	88.3(5)	N(4)–Zn(2)–O(3)	90.1(2)
N(4)–Zn(2)–O(4)	136.5(5)	N(4)–Zn(2)–O(4)	151.6(2)
O(1)–Nd(1)–O(2)	68.3(3)	O(1)–Nd(1)–O(2)	67.32(14)
O(3)–Nd(1)–O(4)	68.9(3)	O(3)–Nd(1)–O(4)	67.31(14)
O(5)–Nd(1)–O(7)	48.9(3)	O(5)–Nd(1)–O(7)	48.89(15)
O(8)–Nd(1)–O(10)	49.1(4)	O(8)–Nd(1)–O(10)	47.94(17)
O(1)–Nd(1)–O(11)	100.1(4)	O(11)–Nd(1)–O(13)	48.62(15)

six oxygen atoms from three bidentate NO_3^- anions, which should be due to the larger π-conjugation effect than that of $\mathbf{H_2L^1}$ in complex **1**. The Nd-O bond lengths vary from 2.409(4) to 2.697(6) Å, and the bond length from coordinated oxygen atoms of NO_3^- anions is slightly longer. The respective solvate molecules (H_2O or Et_2O) of **1** or **5** are not bound to the framework and they exhibit no observable interactions with the host structure.

For the two representative complexes **1** and **5**, their room temperature ^{1}H NMR spectra in CD_3CN are stable and exhibit large shifts (δ from 11.00 to −4.90 ppm for **1** and from 13.11 to −5.23 ppm for **5**) of the proton resonances due to the Nd^{3+}-induced shift, significantly spread relative to those of the respective free $\mathbf{H_2L^1}$ (δ from 8.43 to 3.90 ppm) or $\mathbf{H_2L^2}$ (δ from 8.69 to 6.89 ppm) ligand and the respective precursor **[Zn(L^1)(Py)]** (δ from 8.60 to 3.72 ppm) or **[Zn(L^2)(Py)]** (δ from 9.02 to 6.52 ppm). The ESI-MS spectra of the Zn_2Ln complexes (**1–4**) also support the formula of a trinuclear

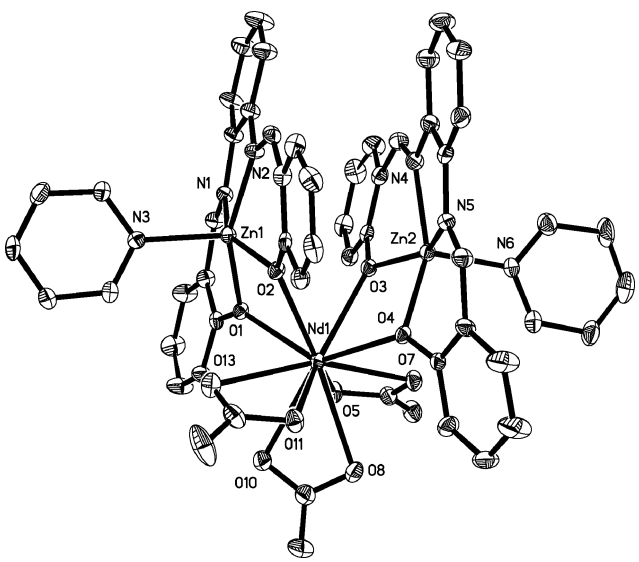

Fig. 2 Perspective drawing of compound **5**, H atoms and solvates are omitted for clarity.

molecule. For the four complexes, the respective ESI-MS spectra exhibit peaks at m/z 1152.82 (**1**), 1181.62 (**2**), 1175.84 (**3**) or 1165.83 (**4**), corresponding to the major species ($[Zn_2(L^1)_2(Py)_2Ln(NO_3)_3\text{-}H]^+$), and indicating that this discrete molecule exists in dilute MeCN solution. And for the four complexes (**5–8**), the ESI-MS spectra of the respective Zn_2Ln complexes also exhibit peaks at m/z 1248.91 (**5**), 1277.71 (**6**), 1271.93 (**7**) or 1261.92 (**8**), corresponding to the major species ($[Zn_2(L^2)_2(Py)_2Ln(NO_3)_3\text{-}H]^+$), and also shows the existence of the discrete molecules in MeCN solution.

Photophysical properties

The photophysical properties of $\mathbf{H_2L^1}$, **[Zn(L^1)(Py)]** and complexes **1–4** have been examined in MeCN solution at room temperature. Selected data are summarized in Table 3 and Fig. 3–5. As shown in Fig. 3, similar ligand-centered solution absorption spectra of complexes **1–4** (228–230, 258–262 and 331–343 nm) in the UV-vis region are observed, red-shifted upon coordination to metal ions as compared to that of the free Salen-type Schiff-base ligand $\mathbf{H_2L^1}$ (213, 255 and 315 nm), while similar to that of the **[Zn(L^1)(Py)]** precursor (227, 264 and 356 nm) with the lowest energy absorption peak being blue-shifted by 15–25 nm. The molar absorption coefficients of complexes **1–4** in all three bands are more than two orders of magnitude larger than that of the free $\mathbf{H_2L^1}$ ligand due to the involvement of two energy donors. For complexes **1–3**, very weak visible emission bands (452 nm, τ = 1.98 ns for **1**; 447 nm, τ = 1.81 ns for **2**; 449 nm, τ = 2.69 ns for **3**) with low quantum yields ($\Phi_{em} < 10^{-5}$) are observed in dilute MeCN solution at room temperature, which can be assigned to the π–π* transitions of the $\mathbf{H_2L^1}$ Schiff-base ligand. In addition to the weak visible emission, as shown in Fig. 4, photo excitation of the antennae in the range of 200–400 nm (λ_{ex} = 339 nm for **1**, λ_{ex} = 360 nm for **2** and λ_{ex} = 360 nm for **3**) gives rise to the characteristic ligand-field splitting emissions of the Nd(III) ion ($^4F_{3/2} \rightarrow {}^4I_{j/2}, j$ = 9, 11, 13), the Yb(III) ion ($^2F_{5/2} \rightarrow {}^2F_{7/2}$) and the Er(III) ion ($^4I_{13/2} \rightarrow {}^4I_{15/2}$) in the NIR region. For **1**, the emissions at 879, 1064 and 1338 nm can be assigned, respectively to $^4F_{3/2} \rightarrow {}^4I_{9/2}$, $^4F_{3/2} \rightarrow {}^4I_{11/2}$ and $^4F_{3/2} \rightarrow {}^4I_{13/2}$ transitions of the Nd(III) ion. For complexes **2** and **3**, the emissions at 976 and 1460 nm can be assigned to the $^2F_{5/2} \rightarrow {}^2F_{7/2}$ transition of the Yb(III) ion and $^4I_{13/2} \rightarrow {}^4I_{15/2}$ transition of the Er(III) ion, respectively. The excitation spectra of complexes **1–3**, monitored at the respective NIR emission peak (1064 nm for **1**, 976 nm for **2** or 1460 nm for **3**) are similar to those monitored at the respective weak visible emission peak, which clearly demonstrates that both the visible and NIR emissions are originated from the same π–π* transitions of the $\mathbf{H_2L^1}$ Schiff-base ligand, and together with the decrease of visible emissions, suggests that the energy transfer from the same antenna to these three Ln(III) ions takes place efficiently.[31] For complexes **1–2**, their respective luminescent decay curves obtained from time-resolved luminescent experiments can be fitted mono-exponentially with lifetimes in microsecond range (2.69 μs for **1** or 13.81 μs for **2**) and the intrinsic quantum yield (1.08% for **1** or 0.69% for **2**) of Ln(III) emission may be estimated by $\Phi_{Ln} = \tau_{obs}/\tau_0$, where τ_{obs} is the observed emission lifetime and τ_0 is the "neutral lifetime", *viz.*

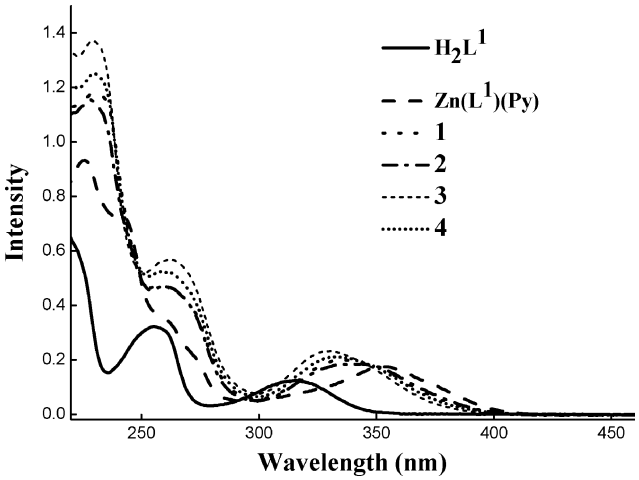

Fig. 3 UV-Vis spectra of $\mathbf{H_2L^1}$, **[ZnL^1(Py)]** and complexes **1–4** in MeCN solution at 2×10^{-5} M at room temperature.

0.25 and 2.0 ms for the Nd(III) and Yb(III) ions, respectively.[32] Due to the limitation of our instrument, we were unable to determine the τ_{obs} for the Er(III) ion and thus could not estimate Φ_{Ln} for the Er(III) ion, though strong NIR emission of the Er(III) ion is observed for complex **3**. The efficiencies of both **1** and **2** are distinctively higher than those of binuclear ZnLn Schiff-base complexes,[22] which should result from the involvement of two energy donors enhancing the sensitization process. As to the higher efficiency of **1** than that of **2**, it should be due to the quantity of accepting levels of the Nd(III) ion while there is only one for the Yb(III) ion. The free $\mathbf{H_2L^1}$ or its **[Zn(L^1)(Py)]** complex do not exhibit NIR luminescence under the same conditions, but display the typical strong luminescence (426 or 453 nm)[21] of Schiff-base ligands in the visible region (Fig. 5).

As a reference compound, complex **4** allows the study of the antenna luminescence in the absence of energy transfer, because the Gd(III) ion has no energy levels below 32 000 cm^{-1}, and therefore cannot accept any energy from the antenna excited state (π*).[33] In dilute MeCN solution at room temperature or 77 K, **4** displays a strong antenna fluorescence

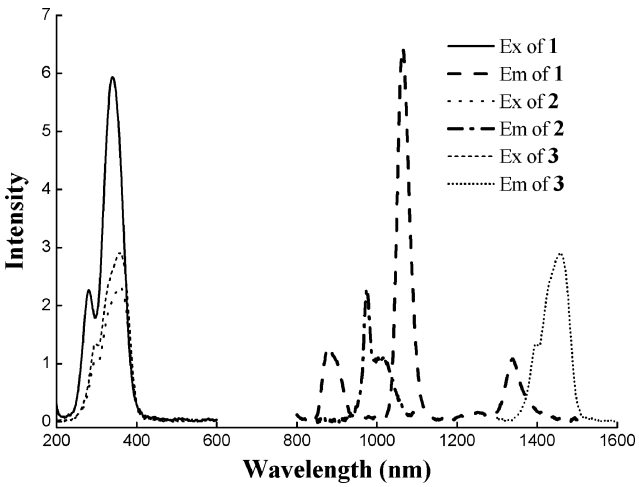

Fig. 4 NIR emission and excitation spectra of complexes **1–3** in MeCN solution at 2×10^{-5} M at room temperature.

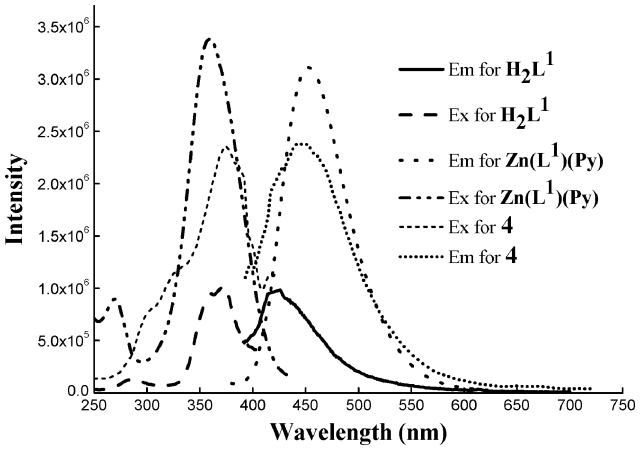

Fig. 5 Visible emission and excitation spectra of H_2L^1, $[Zn(HL^1)(Py)]$ and complex **4** in MeCN solution at 2×10^{-5} M at room temperature.

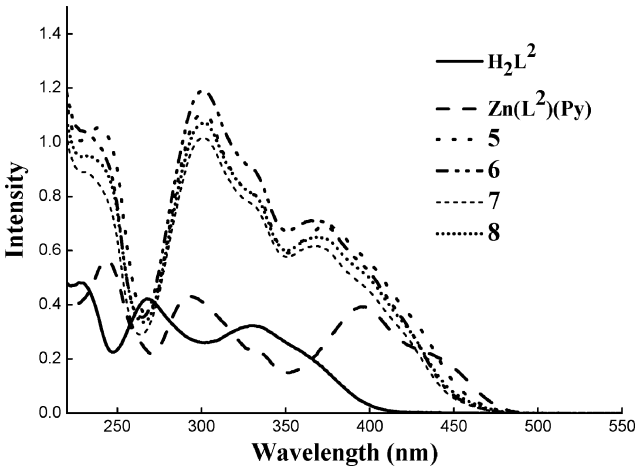

Fig. 6 UV-Vis spectra of H_2L^2, $[ZnL^2(Py)]$ and complexes **5–8** in MeCN solution at 2×10^{-5} M at room temperature.

which has a stronger luminescent intensity, higher quantum yield (1.62×10^{-5}) and slightly longer luminescence lifetime (3.42 ns at room temperature, 5.67 ns and 7.47 ms at 77 K) than that of the antenna luminescence in the other three complexes (**1–3**). This shows that the sensitization of the NIR luminescence should arise from both the ^{1}LC and the ^{3}LC excited state of the ligand at low temperature. Titration (as shown in Fig. 1–3s, ESI†) of the precursor **[Zn(L^1)(Py)]** with $Nd(NO_3)_3$ in dilute MeCN solution shows that the low energy absorption bands exhibit an obvious blue shift to higher energy with concomitant quenching of the **[Zn(L^1)(Py)]** chromophore-based visible luminescence and a gradual increase of NIR emissions upon gradual addition of $Nd(NO_3)_3$. If the antenna luminescence lifetime of **4** is to represent the excited-state lifetime in the absence of energy transfer, the energy transfer rate (k_{ET}) in the complexes **1–3** can thus be calculated from $k_{ET} = 1/\tau_{ZnLn} - 1/\tau_{ZnGd}$, where τ = luminescence lifetime.[34] The calculated rate of the energy transfer process in **1** (2.13×10^8 s^{-1}) is slightly lower than that of **2** (2.60×10^8 s^{-1}), while higher than that of **3** (0.79×10^8 s^{-1}), which may result from the difference of the spectral overlap of the emission of the same antenna and the absorption of the Ln(III) complexes.[35] Although insufficient NIR luminescence information was obtained for **3**, it is noteworthy that the strong NIR emission of the Er(III) ion is unambiguously observed, different from the result of the reported symmetrically phenylene-bridged Schiff-base ZnEr complexes,[22c] which rendered the NIR emission of the Er(III) ion too weak to be observed. The reason should be due to the formation of the trinuclear Zn_2Er molecule for the matching of the donating (antenna) and the receiving (Er(III) ion) levels.[36] On the other hand, the occupation of **Py** groups at the axial positions of Zn(II) ions has ensured that the coordination sphere of Ln^{3+} ions is filled by the Schiff-base and the bidentate nitrate ligands, avoiding luminescent quenching[23] from OH-, CH- or NH-containing solvents around the lanthanide ions in complexes **1–3**.

By extension of the conjugation through changing the linker from ethylene to phenylene (H_2L^1 to H_2L^2), as shown in Table 3 and Fig. 6–8, the absorption spectra of the **[Zn(L^2)(Py)]** precursor and complexes **5–8** are all red shifted relative to the complexes of H_2L^1 (precursor **[Zn(L^1)(Py)]** and **1–4**) and the free H_2L^2 ligand. For the **[Zn(L^2)(Py)]** precursor, the emission maximum is red shifted by about 50 nm, however, its quantum yield is lower than that of the corresponding ethylene-linked precursor (**[Zn(L^1)(Py)]**). This may be due to the fact that the **[Zn(L^2)(Py)]** precursor has a stronger

Table 3 The photophysical properties of H_2L^1, $[ZnL^1(Py)]$ and complexes **1–4** or H_2L^2, $[ZnL^2(Py)]$ and complexes **5–8** at 2×10^{-5} M in absolute MeCN solution at room temperature

Compound	Absorption λ_{ab}/nm (log[ε/dm^{3}mol^{-1} cm^{-1}])	Excitation λ_{ex}/nm	Emission λ_{em}/nm (τ, $\Phi \times 10^{-5}$)
H_2L^2	213(0.70), 255(0.32), 315(0.12)	287, 372	426(s)
$[ZnL^1(Py)]$	227(0.93), 264(0.31), 356(0.17)	270, 360	453(s, 1.56 ns, 36.59)
1	230(1.18), 259(0.47), 336(0.20)	281, 339	452(w, 1.98 ns, $<10^{-2}$), 879 (2.69 μs) 1064, 1338
2	228(1.16), 258(0.47), 343(0.18)	299, 360	447(w, 1.81 ns, $<10^{-2}$), 976 (13.81 μs)
3	229(1.37), 262(0.57), 331(0.23)	300, 360	449(w, 2.69 ns, $<10^{-2}$), 1460
4	230(1.25), 258(0.52), 333(0.21)	301, 375	445(s, 3.42 ns, 1.62) 437(s, 5.67 ns, 77 K), 493(s, 7.47 ms, 77 K)
H_2L^2	227(0.48), 268(0.42), 331(0.32)	320, 331	456(s)
$[ZnL^2(Py)]$	243(0.57), 293(0.43), 397(0.39)	365, 454	506(s, 1.41 ns, 17.92)
5	241(1.05), 301(1.10), 375(0.69)	366, 416	508(m, 3.09 ns, 4.8×10^{-2}), 873 (1.44 μs), 1061, 1335
6	237(1.00), 301(1.19), 369(0.71)	357, 418	507(m, 1.44 ns, 2.6×10^{-2}), 976(6.75 μs)
7	234(0.88), 301(1.02), 370(0.62)	360, 417	508(m, 5.55 ns, 5.7×10^{-2})
8	235(0.95), 302(1.07), 370(0.65)	356, 468	508(s, 7.98 ns, 0.63), 496 (s, 11.45 ns, 77 K)

non-radiative relaxation through internal conversion (IC) or intersystem crossing (ISC) than that of the **[Zn(L^1)(Py)]** precursor. For complexes **5–6** in dilute MeCN solution at room temperature, the weakened visible emissions and the characteristic emissions of the Nd(III) ion ($^4F_{3/2} \rightarrow {}^4I_{j/2}$, j = 9, 11, 13) and the Yb(III) ion ($^2F_{5/2} \rightarrow {}^2F_{7/2}$) in the NIR regions (as shown in Fig. 7) also suggest that the sensitization from the same antenna to these two Ln(III) ions takes place efficiently. Their respective luminescent decay curve obtained from time-resolved luminescent experiments can be fitted mono-exponentially with time constants in the microsecond range (1.44 μs for **5** or 6.75 μs for **6**). It is worth noting that unlike the ethylene-linked complex **3**, characteristic NIR emission of the Er(III) ion for complex **7** cannot be observed. Through further investigation on the emission of the reference compound **8**, especially at 77 K, the nanosecond luminescence lifetime (11.45 ns) shows that the sensitization procedure for the phenylene-linked complexes should result from the ^{1}LC excited state without the ^{3}LC excited state of the **H$_2$L^2** ligand. This shows that the strength of the ISC procedure helps to enhance the sensitization of NIR luminescence of Ln^{3+} ions, which is further proved by the slightly lower estimated intrinsic quantum yields (0.58% for **5** and 0.34% for **6**) than those of the corresponding trinuclear complexes (**1** and **2**). Using the antenna luminescence lifetime of **8** as the excited-state lifetime in the absence of energy transfer, **6** has the highest calculated energy transfer rate (k_{ET} = 5.69 × 10^8 s^{-1}) as compared with **5** (k_{ET} = 1.98 × 10^8 s^{-1}) and **7** (k_{ET} = 0.55 × 10^8 s^{-1}). Upon formation of complex **5** (as shown in Fig. 4–6s, ESI†) from the precursor **[Zn(L^2)(Py)]** with $Nd(NO_3)_3$ in dilute MeCN solution, all the low energy absorption bands are also distinctly blue-shifted, while the **[Zn(L^2)(Py)]** chromophore-based visible luminescence is just partially quenched indicating a lower energy transfer efficient relative to that of complex **1**, despite the gradual increase of NIR emissions upon gradual addition of $Nd(NO_3)_3$. The observed differences from the formation of complexes **1** and **5** can be attributed to the difference in the molecular vibration properties and electronic densities of the electronic states between the ethylene- and phenylene-linked Salen-type complexes, endowing the unobserved phosphorescence in the phenylene-linked complex **5** rationalized as ineffective spin–orbit coupling (SOC) and FCF-controlled (Franck–Condon factor) $S^1 \rightarrow T^1$ ISC, through which the Nd^{3+} sensitization in **1** or **5** was *via* both ^{1}LC and ^{3}LC states or only ^{1}LC at 77 K, respectively, in agreement with the result of *ab initio* calculations[22c] for the ethylene- and phenylene-linked Salen-type binuclear complexes.

Conclusion

The simple Salen-type Schiff-base ligands **H$_2$L^1** and **H$_2$L^2**, without the outer O_2O_2 portion, can bind to both 3d and 4f ions, giving the construction of Zn_2Ln hetero-trinuclear complexes **1–8** with two energy donors for the sensitization of Ln^{3+} ions. The results of their photophysical studies shows that the strong and characteristic NIR luminescence with emissive lifetimes in microsecond ranges, have been sensitized from the excited state (^{1}LC and ^{3}LC or only ^{1}LC) of the ligand, whereas the ligand-centered visible luminescence is mostly quenched because of quite effective intramolecular energy transfer from the ligand-centered excited state of the Zn(II)–Schiff base complex to the Ln(III) ions. The specific design of Zn-coordinated Schiff-base ligands for facilitating the NIR sensitization is now under way.

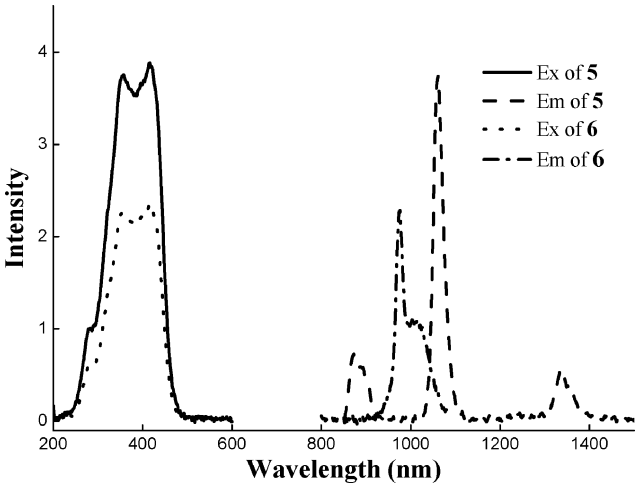

Fig. 7 NIR emission and excitation spectra of complexes **5–6** in MeCN solution at 2 × 10^{-5} M at room temperature.

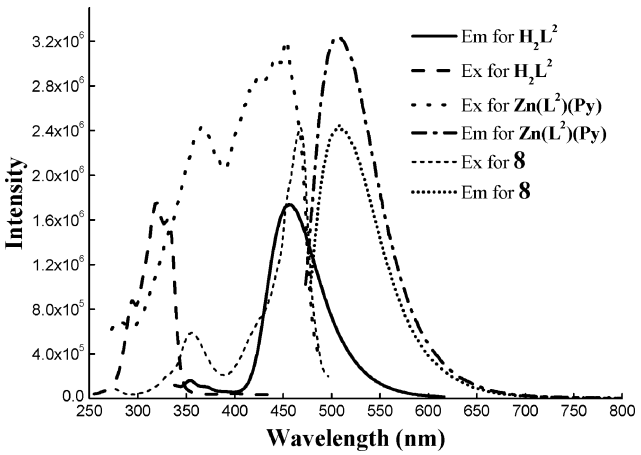

Fig. 8 Visible emission and excitation spectra of **H$_2$L^2**, **[Zn(HL^2)(Py)]** and complex **8** in MeCN solution at 2 × 10^{-5} M at room temperature.

Experimental

All chemicals were commercial products of reagent grade and were used without further purification. Elemental analyses were performed on a Perkin-Elmer 240C elemental analyzer. Infrared spectra were recorded on a Nicolet Nagna-IR 550 spectrophotometer in the region 4000–400 cm^{-1} using KBr pellets. ^{1}H NMR spectra were recorded on a JEOL EX270 spectrometer with $SiMe_4$ as internal standard in CD_3CN at room temperature. ESI-MS was performed on a Finnigan LCQ^{DECA} XP HPLC-MS$_n$ mass spectrometer with a mass to charge (m/z) range of 4000 using a standard electrospray ion source and CH_3CN as solvent. Electronic absorption spectra

in the UV-Vis region were recorded with a Cary 300 UV spectrophotometer, and steady-state visible fluorescence, PL excitation spectra on a Photon Technology International (PTI) Alphascan spectrofluorometer and visible decay spectra on a pico-N_2 laser system (PTI Time Master). The quantum yield of the visible luminescence for each sample was determined by the relative comparison procedure, using a reference of a known quantum yield (quinine sulfate in dilute H_2SO_4 solution, $\Phi_{em} = 0.546$). NIR emission and excitation in solution were recorded by PTI QM4 spectrofluorometer with a PTI QM4 Near-Infrared InGaAs detector.

Syntheses

H_2L^2 or H_2L^2 (H_2L^2: *N*,*N*′-bis(salicylidene)ethylene-1,2-diamine; H_2L^2: *N*,*N*′-bis(salicylidene)phenylene-1,2-diamine). Schiff base H_2L^1 or H_2L^2 was obtained with salicylaldehyde (4.2 ml, 40 mmol) and 1,2-diaminoethane (1.4 ml, 20 mmol) or 1,2-diaminobenzene (2.2 g, 20 mmol) in absolute MeOH or EtOH, respectively, according to a well-established procedure from the literature.[37] For H_2L^1: Yield: 4.0 g, 76%. Calc. for $C_{16}H_{16}O_2N_2$: C, 71.62; H, 6.01; N, 10.44%; found: C, 71.68; H, 6.06; N, 10.53%. ^{1}H NMR (400 MHz, CD_3CN): δ (ppm) 13.34 (s, 2H), 8.43 (s, 2H), 7.29 (m, 4H), 6.83 (m, 4H), 3.90 (s, 4H). For H_2L^2: Yield: 5.8 g, 91%. Calc. for $C_{20}H_{16}O_2N_2$: C, 75.93; H, 5.10; N, 8.85%; found: C, 75.96; H, 5.06; N, 8.93%. ^{1}H NMR (400 MHz, CD_3CN): δ (ppm) 13.02 (s, 2H), 8.69 (s, 2H), 7.45 (m, 2H), 7.34 (m, 2H), 7.29 (m, 4H), 6.89 (m, 4H).

[ZnL^1(Py)] or [ZnL^2(Py)]. To a stirred solution of H_2L^1 (0.540 g, 2.0 mmol) or H_2L^2 (0.640 g, 2.0 mmol) in absolute MeOH (20 ml) or EtOH (20 ml), $Zn(OAc)_2{\cdot}2H_2O$ (0.440 g, 2.0 mmol) and 4.0 ml pyridine (**Py**) were added separately, and the final respective mixture was heated under reflux for 5 h. The respective insoluble precipitate was filtered out, washed with MeOH or EtOH and $CHCl_3$, and dried under vacuum. **[ZnL^1(Py)]** or **[ZnL^2(Py)]** was isolated as a yellow or an orange solid, respectively. For **[ZnL^1(Py)]**: yield: 0.62 g, 76%. Calc. for $C_{21}H_{19}O_2N_3Zn$: C, 61.40; H, 4.66; N, 10.23%; found: C, 61.35; H, 4.72; N, 10.14%. ^{1}H NMR (400 MHz, CD_3CN): δ (ppm) 8.60 (s, 2H), 8.43 (s, 2H), 7.42 (d, 1H), 7.26 (t, 2H), 7.14 (m, 2H), 6.83 (m, 2H), 6.61 (d, 2H), 6.42 (m, 2H), 3.72 (s, 4H). IR (KBr, cm^{-1}): 3050 (w), 2948 (w), 1652 (s), 1632 (vs), 1600 (m), 1530 (m), 1468 (m), 1450 (s), 1391 (m), 1338 (m), 1281 (m), 1238 (w), 1188 (m), 1144 (m), 1046 (w), 901 (w), 755 (m), 736 (w), 523 (w). For **[ZnL^2(Py)]**: yield: 0.83 g, 91%. Calc. for $C_{25}H_{19}O_2N_3Zn$: C, 65.44; H, 4.17; N, 9.16%; found: C, 65.38; H, 4.36; N, 9.05%. ^{1}H NMR (400 MHz, CD_3CN): δ (ppm) 9.02 (s, 2H), 8.82 (m, 2H), 7.91 (m, 3H), 7.41 (m, 4H), 7.25 (m, 4H), 6.71 (d, 2H), 6.52 (m, 2H). IR (KBr, cm^{-1}): 3011 (w), 2923 (w), 1612 (vs), 1583 (m), 1529 (m), 1464 (s), 1386 (m), 1317 (w), 1180 (m), 1152 (m), 1036 (w), 970 (w), 917 (w), 849 (w), 799 (w), 750 (m), 532 (w), 507 (w).

[$Zn_2Ln(L^1)_2(Py)_2(NO_3)_3$]·$H_2O$ (Ln = Nd, 1; Ln = Yb, 2; Ln = Er, 3; Ln = Gd, 4). To a stirred suspension of **[ZnL^1(Py)]** (0.082 g, 0.20 mmol) in absolute MeOH (3 ml), a solution of $Ln(NO_3)_3{\cdot}6H_2O$ (0.10 mmol, Ln = Nd, 0.044 g; Ln = Yb, 0.047 g; Ln = Er, 0.046 g; Ln = Gd, 0.045 g) in absolute MeCN (3 ml) was added, and the mixture was refluxed for about 3 h. The respective yellow clear solution was then cooled to room temperature and filtered. Diethyl ether was allowed to diffuse slowly into the respective solution at room temperature and pale yellow microcrystals **1–4** were obtained in about three weeks, respectively. For **1**: yield: 0.068 g, 58%. Calc. for $C_{42}H_{40}N_9O_{14}Zn_2Nd$: C, 43.12; H, 3.45; N, 10.78%; found: C, 43.08; H, 3,66; N, 10.63%. ^{1}H NMR (400 MHz, CD_3CN): δ (ppm) 11.00 (s, 4H), 7.73 (d, 4H), 7.28 (s, 10H), 4.98 (t, 8H), 0.49 (d, 4H), −4.90 (s, 8H). IR (KBr, cm^{-1}): 3446 (b), 3058 (w), 2915 (w), 1647 (vs), 1600 (s), 1550 (m), 1473 (s), 1446 (vs), 1392 (s), 1277 (vs), 1196 (m), 1157 (w), 1126 (w), 896 (m), 762 (s), 700 (m), 563 (w), 502 (w), 460 (w). ESI-MS (CH_3CN) *m*/*z*: 1152.82 (100%), 1089.81 (58%). For **2**: yield: 0.059 g, 49%. Calc. for $C_{42}H_{40}N_9O_{14}Zn_2Yb$: C, 42.09; H, 3.36; N, 10.52%; found: C, 41.95; H, 3.54; N, 10.47%. IR (KBr, cm^{-1}): 3450 (b), 3066 (w), 2921 (w), 1647 (vs), 1601 (s), 1551 (m), 1476 (vs), 1445 (s), 1397 (m), 1279 (vs), 1199 (m), 1157 (w), 1125 (w), 1036 (w), 896 (m), 760 (s), 699 (m), 566 (w), 503 (w), 461 (w). ESI-MS (CH_3CN) *m*/*z*: 1181.62 (100%), 1118.61 (43%). For **3**: yield: 0.061 g, 51%. Calc. for $C_{42}H_{40}N_9O_{14}Zn_2Er$: C, 42.29; H, 3.38; N, 10.57%; found: C, 42.08; H, 3.56; N, 10.41%. IR (KBr, cm^{-1}): 3446 (b), 3058 (w), 2915 (w), 1647 (vs), 1600 (s), 1550 (m), 1473 (s), 1446 (vs), 1392 (s), 1277 (vs), 1196 (m), 1157 (w), 1126 (w), 896 (m), 762 (s), 700 (m), 563 (w), 502 (w), 460 (w). ESI-MS (CH_3CN) *m*/*z*: 1175.84 (100%), 1112.83 (48%). For **4**: yield: 0.063 g, 53%. Calc. for $C_{42}H_{40}N_9O_{14}Zn_2Gd$: C, 42.65; H, 3.41; N, 10.66%; found: C, 42.49; H, 3.576; N, 10.58%. IR (KBr, cm^{-1}): 3416 (b), 3052 (w), 2919 (w), 1649 (vs), 1601 (s), 1548 (m), 1474 (vs), 1446 (s), 1390 (m), 1277 (vs), 1195 (m), 1158 (w), 1125 (w), 896 (m), 759 (s), 701 (w), 561 (w), 498 (w), 460 (w). ESI-MS (CH_3CN) *m*/*z*: 1165.83 (100%), 1102.82 (50%).

[$Zn_2(L^2)_2Nd(Py)_2(NO_3)_3$]·$Et_2O$ (Ln = Nd, 5; Ln = Yb, 6; Ln = Er, 7; Ln = Gd, 8). To a stirred suspension of **[ZnL^2(Py)]** (0.092 g, 0.20 mmol) in absolute EtOH (4 ml), a solution of $Ln(NO_3)_3{\cdot}6H_2O$ (0.10 mmol, Ln = Nd, 0.044 g; Ln = Yb, 0.047 g; Ln = Er, 0.046 g; Ln = Gd, 0.045 g) absolute MeCN (5 ml) was added, and the mixture was refluxed for about 5 h. The respective yellow clear solution was then cooled to room temperature and filtered. Diethyl ether was allowed to diffuse slowly into the respective solution at room temperature and pale yellow microcrystals **5–8** were obtained in about two weeks, respectively. For **5**: yield: 0.107 g, 81%. Calc. for $C_{54}H_{48}N_9O_{14}Zn_2Nd$: C, 49.06; H, 3.66; N, 9.54%; found: C, 49.02; H, 3.75; N, 9.44%. ^{1}H NMR (400 MHz, CD_3CN): δ (ppm) 13.11 (s, 2H), 8.55 (m, 2H), 7.80 (m, 3H), 7.28 (m, 4H), 6.40(m, 4H), 3.32 (d, 2H), −5.23 (m, 2H). IR (KBr, cm^{-1}): 2969 (w), 2923 (w), 1615 (vs), 1585(m), 1547 (m), 1536(m), 1462 (s), 1444(vs), 1385 (m), 1326 (m), 1282 (m), 1254(w), 1182 (m), 1159 (m), 1126 (m), 1037 (m), 986 (w), 917 (m), 793 (w), 751 (s), 695 (w), 605 (w), 535 (m), 490 (m). ESI-MS (CH_3CN) *m*/*z*: 1248.91 (100%), 1185.90 (39%). For **6**: yield: 0.092 g, 68%. Calc. for $C_{54}H_{48}N_9O_{14}Zn_2Yb$: C, 48.01; H, 3.58; N, 9.33%; found: C, 48.12; H, 3.67; N, 9.21%. IR (KBr, cm^{-1}): 2971 (w), 2854 (w), 1615 (vs), 1546 (m), 1514 (m), 1470 (vs), 1386 (m), 1300 (s), 1184 (m), 1156 (m), 1120 (m), 1023 (m), 976 (w), 915 (m), 793 (w), 757 (s), 694 (w), 601 (w),

532 (m), 494 (m). ESI-MS (CH_3CN) m/z: 1277.71 (100%), 1214.70 (55%). For **7**: yield: 0.099 g, 74%. Calc. for $C_{54}H_{48}N_9O_{14}Zn_2Er$: C, 48.22; H, 3.60; N, 9.37%; found: C, 48.14; H, 3.66; N, 9.24%. IR (KBr, cm^{-1}): 2972 (w), 2856 (w), 1615 (vs), 1546 (m), 1522 (m), 1470 (vs), 1386 (m), 1286 (s), 1184 (m), 1156 (m), 1120 (m), 1022 (m), 975 (w), 915 (w), 791 (w), 755 (s), 700 (w), 602 (w), 534 (m), 496 (m). ESI-MS (CH_3CN) m/z: 1271.93 (100%), 1208.92 (41%). For **8**: yield: 0.088 g, 66%. Calc. for $C_{54}H_{48}N_9O_{14}Zn_2Gd$: C, 48.58; H, 3.62; N, 9.44%; found: C, 48.41; H, 3.78; N, 9.37%. IR (KBr, cm^{-1}): 2971 (w), 2854 (w), 1614 (vs), 1546 (m), 1509 (m), 1470 (vs), 1386 (m), 1286 (s), 1183 (m), 1155 (m), 1120 (m), 1020 (m), 976 (w), 914 (m), 793 (w), 757 (s), 693(w), 600 (w), 531 (m), 492 (m). ESI-MS (CH_3CN) m/z: 1261.92 (100%), 1198.91 (46%).

X-Ray crystallography

Single crystals of **1** and **5** of suitable dimensions were mounted onto thin glass fibers. All the intensity data were collected on a Bruker SMART CCD diffractometer (Cu-Kα radiation and λ = 1.54184 Å for **1**, Mo-Kα radiation and λ = 0.71073 Å for **5**) in Φ and ω scan modes. Structures were solved by Patterson methods followed by difference Fourier syntheses, and then refined by full-matrix least-squares techniques against F^2 using SHELXTL.[38] All other non-hydrogen atoms were refined with anisotropic thermal parameters. Absorption corrections were applied using SADABS.[39] All hydrogen atoms were placed in calculated positions and refined isotropically using a riding model. Crystallographic data and refinement parameters for the complexes are presented in Table 1. Relevant atomic distances and bond angles are collected in Table 2. CCDC reference number 725680 (for **1**) and 725681 (for **5**).

Acknowledgements

This work was funded by the National Natural Science Foundation (20871098), the Provincial Key Item of Shaanxi, the Provincial Natural Foundation (2007B03) of Shaanxi, Education Committee Foundation of Shaanxi Province (07JK391), Graduate Cross-discipline Funds (07YJC11) and Graduate Innovation and Creativity Funds (08YZZ48) of Northwest University, Hong Kong Research Grants Council (HKBU 202407 and FRG/06-07/II-16) in P. R. of China, the Robert A. Welch Foundation (Grant F-816), the Texas Higher Education Coordinating Board (ARP 003658-0010-2006) and the Petroleum Research Fund, administered by the American Chemical Society (47014-AC5).

References

1 (*a*) S. Stolik, J. A. Delgado, A. Perez and L. Anasagasti, *J. Photochem. Photobiol., B*, 2000, **57**, 90; (*b*) R. Weissleder and V. Ntziachristos, *Nat. Med.*, 2003, **9**, 123; (*c*) S. Kim, Y. T. Lim, E. G. Soltesz, A. M. De Grand, J. Lee, A. Nakayama, J. A. Parker, T. Mihaljevic, R. G. Laurence, D. M. Dor, L. H. Cohn, M. G. Bawendi and J. V. Frangioni, *Nat. Biotechnol.*, 2004, **22**, 93.
2 (*a*) T. Jüstel, D. U. Wiechert, C. Lau, D. Sendor and U. Kynast, *Adv. Funct. Mater.*, 2001, **11**, 105; (*b*) T.-S. Kang, B. S. Harrison, T. J. Foley, A. S. Knefely, J. M. Boncella, J. R. Reynolds and K. S. Schanze, *Adv. Mater.*, 2003, **15**, 1093; (*c*) A. O' Riordan, R. Van Deun, E. Mairiaux, S. Moynihan, P. Fias, P. Nockemann, K. Binnemans and G. Redmond, *Thin Solid Films*, 2008, **516**, 5098.
3 L. Winkless, R. H. C. Tan, Y. Zheng, M. Motevalli, P. B. Wyatt and W. P. Gillin, *Appl. Phys. Lett.*, 2006, **89**, 111115.
4 J.-C. G. Bünzli and C. Piguet, *Chem. Soc. Rev.*, 2005, **34**, 1048.
5 (*a*) S. Faulkner, B. P. Burton-Pye, T. Khan, L. R. Martin, S. D. Wray and P. J. Skabara, *Chem. Commun.*, 2002, 1668; (*b*) H.-S. He, X.-J. Zhu, A.-X. Hou, J.-P. Guo, W.-K. Wong, W.-Y. Wong, K.-F. Li and K.-W. Cheah, *Dalton Trans.*, 2004, 4064; (*c*) S. J. A. Pope, B. P. Burton-Pye, R. Berridge, T. Khan, P. J. Skabara and S. Faulkner, *Dalton Trans.*, 2006, 2907.
6 (*a*) H.-S. Wang, G.-D. Qian, M.-Q. Wang, J.-H. Zhang and Y.-S. Luo, *J. Phys. Chem. B*, 2004, **108**, 8084; (*b*) D. Imbert, S. Comby, A. S. Chauvin and J. C. G. Bünzli, *Chem. Commun.*, 2005, 1432; (*c*) M.-K. Nah, S.-G. Rho, H. K. Kim and J.-G. Kang, *J. Phys. Chem. A*, 2007, **111**, 11437; (*d*) M. Giraud, E. S. Andreiadis, A. S. Fisyuk, R. Demadrille, J. Pécaut, D. Imbert and M. Mazzanti, *Inorg. Chem.*, 2008, **47**, 3952; (*e*) A. P. S. Samuel, E. G. Moore, M. Melchior, J.-D. Xu and K. N. Raymond, *Inorg. Chem.*, 2008, **47**, 7535.
7 (*a*) J. Zhang, P. D. Badger, S. J. Geib and S. Petoud, *Angew. Chem., Int. Ed.*, 2005, **44**, 2508; (*b*) J. Zhang and S. Petoud, *Chem.–Eur. J.*, 2008, **14**, 1264; (*c*) W. Huang, D.-Y. Wu, D. Guo, X. Zhu, C. He, Q.-J. Meng and C.-Y. Duan, *Dalton Trans.*, 2009, 2081.
8 M. D. Ward, *Coord. Chem. Rev.*, 2007, **251**, 1663.
9 (*a*) D. Imbert, M. Cantnuel, J. C. G. Bünzli, G. Bernardinelli and C. Piguet, *J. Am. Chem. Soc.*, 2003, **125**, 15698; (*b*) S. Torelli, D. Imbert, M. Cantnuel, G. Bernardinelli, S. Delahaye, A. Hauser, J.-C. G. Bünzli and C. Piguet, *Chem.–Eur. J.*, 2005, **11**, 3228.
10 W.-K. Wong, A.-X. Hou, J.-P. Guo, H.-S. He, L.-L. Zhang, W.-Y. Wong, K.-F. Li, K.-W. Chean, F. Xue and T. C. W. Mak, *J. Chem. Soc., Dalton Trans.*, 2001, 3092.
11 S. Akine, T. Taniguchi and T. Nabeshima, *Angew. Chem., Int. Ed.*, 2002, **41**, 4670.
12 (*a*) S. I. Klink, H. Keizer and F. C. J. M. van Veggel, *Angew. Chem., Int. Ed.*, 2000, **39**, 4319; (*b*) D. Guo, C.-Y. Duan, F. Lu, Y. Hasegawa, Q.-J. Meng and S. Yanagida, *Chem. Commun.*, 2004, 1486; (*c*) C. Giansante, P. Ceroni, V. Balzani and F. Vögtle, *Angew. Chem., Int. Ed.*, 2008, **47**, 5422.
13 A. Beeby, R. S. Dickins, S. FitzGerald, L. J. Govenlock, C. L. Maupin, D. Parker, J. P. Riehl, G. Siligardi and J. A. G. Williams, *Chem. Commun.*, 2000, 1183.
14 (*a*) P. B. Glover, P. R. Ashton, L. J. Childs, A. Rodger, M. Kercher, R. M. Williams, L. de Cola and Z. Pikramenou, *J. Am. Chem. Soc.*, 2003, **125**, 9918; (*b*) H.-B. Xu, L.-X. Shi, E. Ma, L.-Y. Zhang, Q.-H. Wei and Z.-N. Chen, *Chem. Commun.*, 2006, 1601; (*c*) X.-L. Li, F.-R. Dai, L.-Y. Zhang, Y.-M. Zhu, Q. Peng and Z.-N. Chen, *Organometallics*, 2007, **26**, 4483; (*d*) H.-B. Xu, L.-Y. Zhang, Z.-H. Chen, L.-X. Shi and Z.-N. Chen, *Dalton Trans.*, 2008, 4664; (*e*) J. Ni, L.-Y. Zhang and Z.-N. Chen, *J. Organomet. Chem.*, 2009, **694**, 339.
15 (*a*) M. Mehlstäubl, G. S. Kottas, S. Colella and L. de Cola, *Dalton Trans.*, 2008, 2385; (*b*) F.-F. Chen, Z.-Q. Bian, B. Lou, E. Ma, Z.-W. Liu, D. B. Nie, Z.-Q. Chen, J. Bian, Z.-N. Chen and C.-H. Huang, *Dalton Trans.*, 2008, 5577.
16 H.-B. Xu, L.-Y. Zhang, J. Ni, H.-Y. Chao and Z.-N. Chen, *Inorg. Chem.*, 2008, **47**, 10744.
17 B. Zhao, X.-Q. Zhao, Z. Chen, W. Shi, P. Cheng, S.-P. Yan and D.-Z. Liao, *CrystEngComm*, 2008, **10**, 1144.
18 Y.-X. Chi, S.-Y. Niu, Z.-J. Wang and J. Jin, *Eur. J. Inorg. Chem.*, 2008, 2336.
19 S. J. A. Pope, B. J. Coe, S. Faulkner and R. H. Laye, *Dalton Trans.*, 2005, 1482.
20 (*a*) J.-P. Costes, F. Dahan, G. Novitchi, V. Arion, S. Shova and J. Lipkowshi, *Eur. J. Inorg. Chem.*, 2004, 1530; (*b*) R. Gheorghe, P. Cucos, M. Andruh, J.-P. Costes, B. Donnadieu and S. Shova, *Chem.–Eur. J.*, 2006, **12**, 187.
21 S. Mizukami, H. Houjou, K. Sugaya, E. Koyama, H. Tokuhisa, T. Sasaki and M. Kanesato, *Chem. Mater.*, 2005, **17**, 50.
22 (*a*) W.-K. Wong, H.-Z. Liang, W.-Y. Wong, Z.-W. Cai, K.-F. Li and K.-W. Cheah, *New J. Chem.*, 2002, **26**, 275; (*b*) W.-K. Lo, W.-K. Wong, J.-P. Guo, W.-Y. Wong, K.-F. Li and K.-W. Cheah, *Inorg. Chim. Acta*, 2004, **357**, 4510; (*c*) W.-K. Lo, W.-K. Wong, W.-Y. Wong, J.-P. Guo, K.-T. Yeung, Y.-K. Cheng, X.-P. Yang

and R. A. Jones, *Inorg. Chem.*, 2006, **45**, 9315; (*d*) X.-P. Yang, R. A. Jones, Q.-Y. Wu, M. M. Oye, W.-K. Lo, W.-K. Wong and A. L. Holmes, *Polyhedron*, 2006, **25**, 271; (*e*) W.-Y. Bi, X.-Q. Lü, W.-L. Chai, J.-R. Song, W.-Y. Wong, W.-K. Wong and R. A. Jones, *J. Mol. Struct.*, 2008, **891**, 450; (*f*) W.-Y. Bi, X.-Q. Lü, W.-L. Chai, J.-R. Song, W.-K. Wong, X.-P. Yang and R. A. Jones, *Z. Anorg. Allg. Chem.*, 2008, **634**, 1795.
23 F. Quochi, R. Orru, F. Cordella, A. Mura, G. Bongiovanni, F. Artizzu, P. Deplanto, M. L. Mercurri, L. Pilla and A. Serpe, *J. Appl. Phys.*, 2006, **99**, 53520.
24 X.-P. Yang, R. A. Jones, V. Lynch, M. M. Oye and A. L. Holmes, *Dalton Trans.*, 2005, 849.
25 W.-K. Wong, X.-P. Yang, R. A. Jones, J. H. Rivers, V. Lynch, W.-K. Lo, D. Xiao, M. M. Oye and A. L. Holmes, *Inorg. Chem.*, 2006, **45**, 4340.
26 X.-Q. Lü, W.-Y. Bi, W.-L. Chai, J.-R. Song, J.-X. Meng, W.-Y. Wong, W.-K. Wong and R. A. Jones, *New J. Chem.*, 2008, **32**, 127.
27 (*a*) X.-P. Yang, R. A. Jones, W.-K. Wong, M. M. Oye and A. L. Holmes, *Chem. Commun.*, 2006, 1836; (*b*) X.-Q. Lü, W.-Y. Bi, W.-L. Chai, J.-R. Song, J.-X. Meng, W.-Y. Wong, W.-K. Wong, X.-P. Yang and R. A. Jones, *Polyhedron*, 2009, **28**, 27.
28 K. C. Gupta and A. K. Sutar, *Coord. Chem. Rev.*, 2008, **252**, 1420.
29 (*a*) X.-P. Yang, R. A. Jones and W.-K. Wong, *Chem. Commun.*, 2008, 3266; (*b*) X.-P. Yang, R. A. Jones and W.-K. Wong, *Dalton Trans.*, 2008, 1676.
30 A. W. Addison, T. N. Rao, J. Reedijk, J. van Rijn and G. C. Verschoor, *J. Chem. Soc., Dalton Trans.*, 1984, 1349.
31 M. Albrecht, O. Osetska, J. Klankermayer, R. Fröhlich, F. Gumy and J. C. G. Bünzli, *Chem. Commun.*, 2007, 1834.
32 M. J. Weber, *Phys. Rev.*, 1968, **171**, 283.
33 W. T. Carnall, P. R. Fields and K. Rajnak, *J. Chem. Phys.*, 1968, **49**, 4443.
34 G. Stein and E. Würzberg, *J. Chem. Phys.*, 1975, **62**, 208.
35 D. L. Dexter, *J. Chem. Phys.*, 1953, **21**, 836.
36 J.-C. G. Bünzli, S. Comby, A.-S. Chauvin and C. D. B. Vandevyver, *J. Rare Earths*, 2007, **25**, 257.
37 (*a*) F. Lam, J.-X. Xu and K. S. Chan, *J. Org. Chem.*, 1996, **61**, 8414; (*b*) P. G. Lacroix, S. D. Bella and I. Ledoux, *Chem. Mater.*, 1996, **8**, 541.
38 G. M. Sheldrick, *SHELXS-97: Program for crystal structure refinement*, University of Göttingen, Göttingen, Germany, 1997.
39 G. M. Sheldrick, *SADABS*, University of Göttingen, Göttingen, Germany, 1996.

